Letter

Robert Kirchner*, Vitaliy A. Guzenko and Helmut Schift

Single-digit 6-nm multilevel patterns by electron beam grayscale lithography

https://doi.org/10.1515/aot-2019-0016
Received January 31, 2019; accepted March 25, 2019; previously published online April 22, 2019

Abstract: We report on the fabrication of very high-resolution discrete four-resist-level grayscale patterns in poly(methyl methacrylate) with just 6-nm step height and down to 32-nm step width using dose-modulated, grayscale electron beam lithography and a low-contrast resist-developer system. This direct pattern writing is important for replication in high-volume manufacturing of diffractive optics. An innovative concept of unexposed auxiliary spacers helped to enhance the discrete character of the multi-level patterns. For pattern step widths between 100 and 32 nm, a transformation toward blazed gratings with increasingly continuous-slope character was obtained. All high-resolution patterns were prepared in a single exposure and development process from an initially about 30-nm thin film. The pattern roughness due to a relatively large polymer molecular weight was reduced using selective thermal annealing with only minimally affecting the global pattern shape by reflow. The results will enable further approaches toward single-digit vertical and prospectively single-digit lateral resolution grayscale patterns.

Keywords: diffractive; high resolution; optics; polymer replication; precision.

Discrete and continuous slope diffractive optical elements can be made by several micro- and nano-fabrication methods. The most common ones are (i) multiple consequent lithography, developing and pattern-transfer steps requiring precise overlay between each binary lithography step [1, 2], as well as (ii) grayscale lithography involving dose modulation in the radiation-sensitive resist. Dose modulation can be realized by either grayscale optical masks (e.g. halftone-like masks [3, 4], transmission modulation masks [5, 6]) or by modulation during direct writing with laser [7], electron [8–13] or ion beam [14] lithography. Interference lithography is another maskless method for regular and advanced continuous profile patterns and can be applied from infrared [15] to extreme ultraviolet (EUV) wavelength regime [16]. Especially for high-resolution and demanding patterns, electron or ion beam lithography is the method of choice.

High-precision and high-resolution diffractive optics are important for large divergence optics, beam shape control and aerial image formation. Applications are, for example, data transmission and barcode scanners [2], optical tweezers [17], optical lithography in the UV [18] and EUV range [19], hybrid optics [2, 20–22], nanofluidics [14], hierarchical surfaces [23], astronomical gratings [24] and spectrometers [25]. Grayscale electron beam lithography has been applied across scales from sub-10-µm [26] down to sub-100-nm feature height and width before [24] (Figure 1). This work demonstrates for the first time sub-10-nm step height. The obtained step pattern is universal and independent of the used resist-developer system for designs with the same step width-to-step height ratio [12]. This can be explained by development rates. Grayscale profiles only rely on differences in development rates due to differences in molecular weight arising from the dose-modulated exposure. For example, independent of the used resist-developer system, a step pattern with a remaining 50% step and 0% step (cleared) of the original resist film will always be the same. Independent of the used resist-developer, the development rate for the 50% step is always two times slower compared to the 0% step resulting in the same grayscale profile for a given step width-to-step height ratio.

For fabrication, we used a 100-kV Gaussian spot electron beam writer (VISTEC EBPG 5000+, Raith GmbH, Dortmund, Germany) with 1-nA beam current (400-µm

***Corresponding author: Robert Kirchner,** Paul Scherrer Institute, Laboratory for Micro- and Nanotechnology, 5232 Villigen PSI, Switzerland; and Technische Universität Dresden, Institute of Semiconductors and Microsystems, 01062 Dresden, Germany, e-mail: robert.kirchner@tu-dresden.de
Vitaliy A. Guzenko and Helmut Schift: Paul Scherrer Institute, Laboratory for Micro- and Nanotechnology, 5232 Villigen PSI, Switzerland

www.degruyter.com/aot

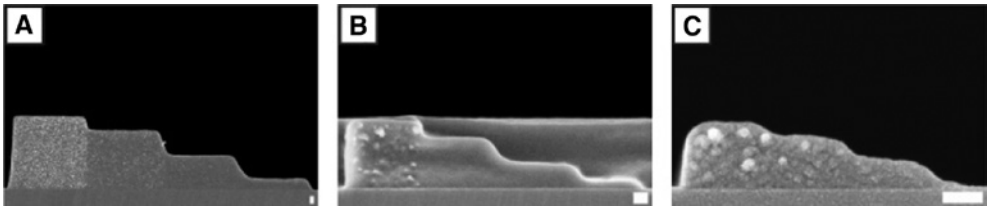

Figure 1: Scanning electron micrographs of cross sections through four-resist-level grayscale patterns fabricated in 100 kg/mol PMMA prepared from different initial films of (A) 2000 nm, (B) 500 nm and (C) 200 nm (scale bar, 100 nm). The notable granularity, especially of the highest (= unexposed) step, is due to the relative large molecular weight compared to the other steps.

aperture: spot size ~10 nm). Samples were exposed according to a dose mapping and three-dimensional (3D) proximity correction using a commercial software package (BEAMER, GenISys GmbH, Taufkirchen, Germany) and previously measured contrast curves for blank silicon samples with about 28-nm-thin poly(methyl methacrylate) (PMMA 120k, micro resist technology GmbH, Berlin, Germany) spun-on films (Figure 2). The samples were post-apply baked on a hotplate for 2 min at 140°C. The molecular weight of the PMMA was about 100 kg/mol, and the glass transition temperature was about 122°C [27]. Exposed samples were developed in a mixture of methyl isobutyl ketone (MIBK) and isopropyl alcohol (IPA) in a ratio of MIBK:IPA 1:3 at 20°C for typically 50–60 s (endpoint detection via atomic force microscopy [AFM]). Samples were immediately rinsed for 30 s in IPA after development. The contrast of the resist-developer process is determined by the ratio of the dose required to completely remove the resist to the threshold dose where resist removal sets in. High contrast means a steep decay of the contrast curve (cf. Figure 2). Figure 2 is considered to be a low-contrast system in this experimental setup and in the frame of grayscale lithography. Even though low-contrast systems have drawbacks in feature definition accuracy (corner rounding, tapered sidewalls), the dose control is more relaxed and dose variations do affect pattern shape much less compared to high-contrast systems. This variation sensitivity is especially important for large area writing involving multiple writing field stitching, where slightest dose variations become quite prominent especially in grayscale patterning.

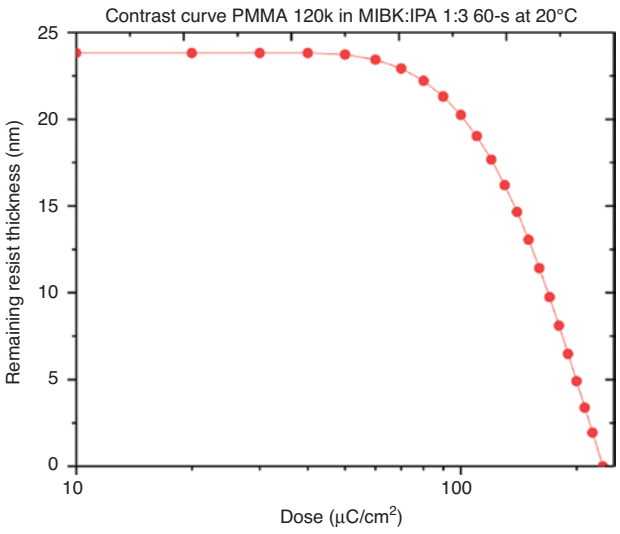

Figure 2: Contrast curve of the low-contrast system: 24-nm PMMA 120k in MIBK:IPA 1:3 for 60-s development at 20°C (contrast $\gamma = 1.71$).

Single-digit vertical resolution patterns with large step width-to-step height ratio can be fabricated with great accuracy compared to the design file (Figure 3A). Deviations of the average profile of line scans from the design file are mainly due to the used low-contrast developer-resist system (step-to-step sidewall taper) as well as the large molecular weight giving rise to surface and line edge roughness. Earlier work showed that the lower-molecular-weight steps (larger dose) tend to have large development-induced surface roughness [25, 27]. The same is visible in Figure 3A. For reduced step widths, the precision due to the low-contrast system degrades, and the roughness becomes more dominant even though being at a constant level (Figure 3B and C). The experimental deviation of the total height of the highest step from the design is mainly due to local variations in the initial film thickness as well as proximity effects. This means, because of physical limitations, these unexposed regions still receive a non-negligible dose leading to a certain development. An additional feature that is visible is the typical trenching between two steps that increases at higher exposure dose levels. We attribute this to a dose variation due to data fracturing at the software level.

Figure 3C indicates the problem of vanishing step definition accuracy due to the low contrast. This can be partly compensated by inserting unexposed regions (high-molecular-weight) acting as a separation between two exposed regions. Because of the low contrast, the exposed regions

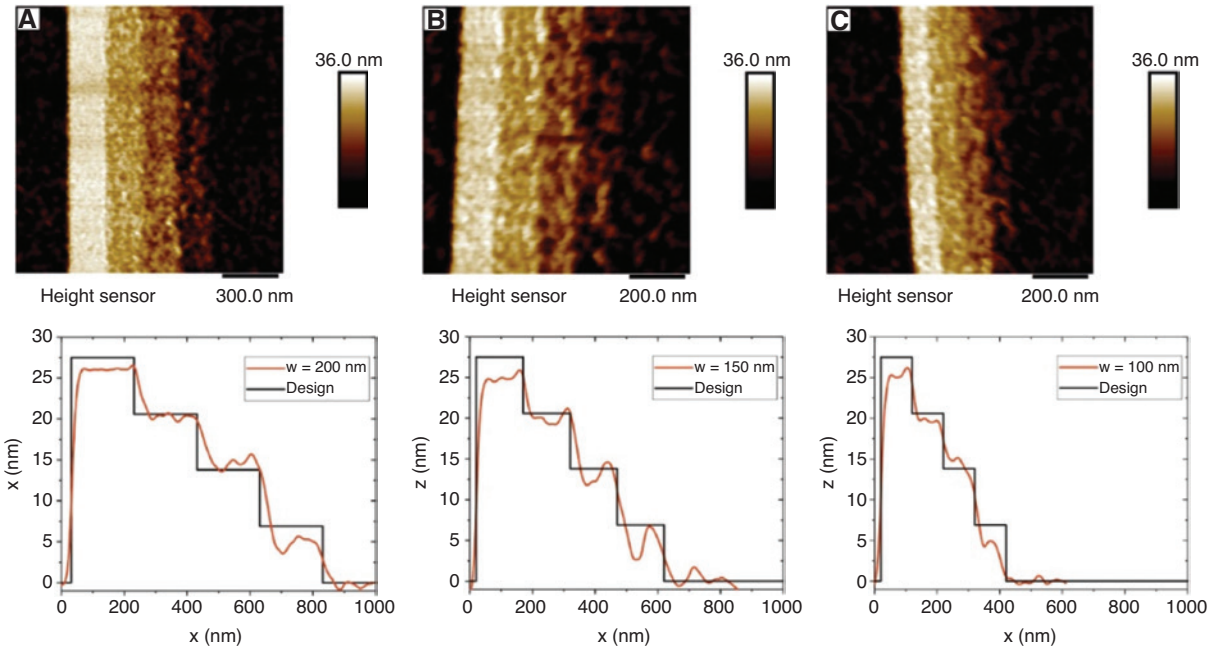

Figure 3: AFM average of multiple line scans of different grayscale patterns with different step widths: (A) 200-nm, (B) 150-nm and (C) 100-nm wide steps prepared from initially 28-nm-thin PMMA films and yielding 6-nm vertical step height resolution. (top row: large-area AFM scan, bottom row: full field average of single-line AFM scans; note: AFM height sensor signal was used).

have similar molecular weight and, thus, development rates. As a result, the relatively strong lateral compared to the vertical development results in a feature definition loss. However, unexposed sections between each step that were originally introduced by Guzenko et al. can reduce the lateral development [28] (Figure 4A). The 30-nm spacing (Figure 4C) improved the desired discrete pattern profile compared to the design without a gap (Figure 4B) as demonstrated for a roughly 900-nm-high pattern with four equally high sized and about 500–750-nm-wide steps. The exposure with gaps features an almost flat step profile until the step edge. The step angle itself cannot be correctly measured due to the AFM tip shape. The empirical, constant value of 30 nm is a good compromise between profile improvement and minimal data preparation effort.

For further tested higher-resolution four-resist-step designs, only blazed gratings were obtained with a significant erosion in the unexposed area (Figure 5). The non-existing flat top in these unexposed areas indicates the process and material limitation for the used experimental setup. Between 100- and 32-nm step width, the continuous character of the obtained pattern steadily increased. This is especially visible when comparing single line

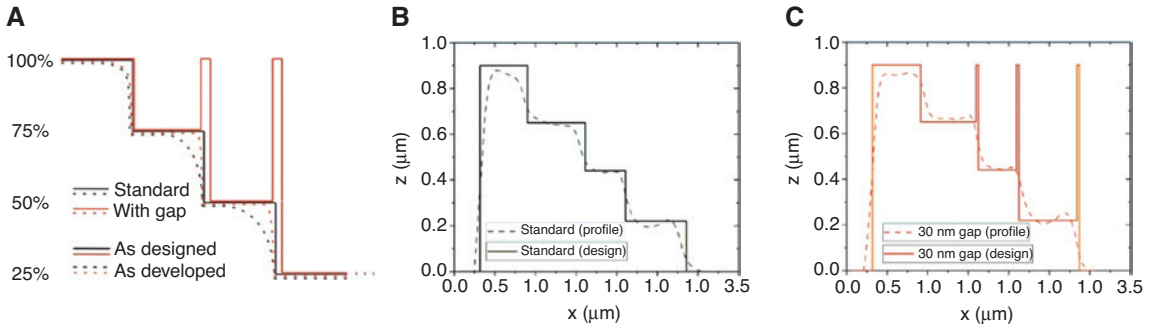

Figure 4: (A) Schematic for an improved step-to-step angle as well as sharper profiles by using unexposed segments between different steps reducing the lateral development. Comparison of single line scans of an (B) exposure without gap (standard) and (C) exposure of the same pattern but using 30-nm unexposed gaps between selected steps, giving a clear profile shape improvement especially for the exposed steps (note: no realistic vertical step edges due to AFM tip shape effect – profile convolution).

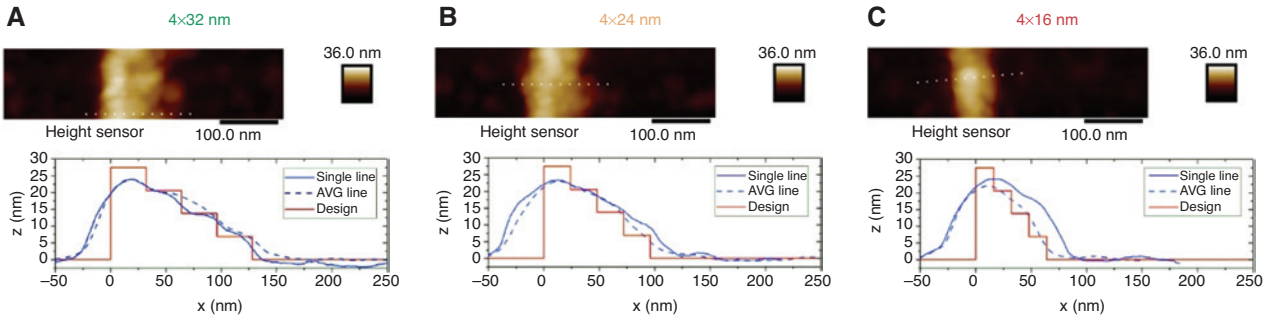

Figure 5: Comparison of three high-resolution exposures with (A) four steps each 32 nm wide, (B) four steps each 24 nm wide and (C) four steps each 16 nm wide (note: all data are single line scans [while dotted line] and line-averaged profiles for the shown images; AFM height sensor signal was used).

scans: the 4×32-nm pattern can be considered as the highest obtained resolution with some remaining discrete pattern character. Also, the line edge roughness, due to a relatively large molecular weight of the PMMA, sets a clear limitation for this process. A further enhancement with unexposed gaps might improve the discrete pattern character; however, the erosion of the unexposed pattern is already quite significant, and the enhancement effect will be, thus, quite limited.

The related and inherent surface roughness of the steps could be smoothed by applying a thermal annealing on a hotplate of 110°C and 120°C for about 20 min (Figure 6). The applied temperature still being below the glass transition temperature of the PMMA pattern was sufficient to trigger local nanoscopic polymer rearrangement, while larger-scale microscopic reflow of the pattern was avoided. Another reason for preserving the microscopic structure is the large step width-to-step height ratio that would require a relatively large time for a significant deformation of the steps due to the lateral polymer flow. The lower temperature of 110°C was more suited for keeping the line edge roughness low.

The used PMMA has been shown to be stable enough to allow for replication of daughter molds directly from the PMMA to preserve the pattern fidelity [29]. Considering the used pattern size, we see this as an alternative to pattern transfer [30].

In conclusion, we have demonstrated the ability to apply vertical and lateral high-resolution grayscale electron beam lithography for the fabrication of discrete

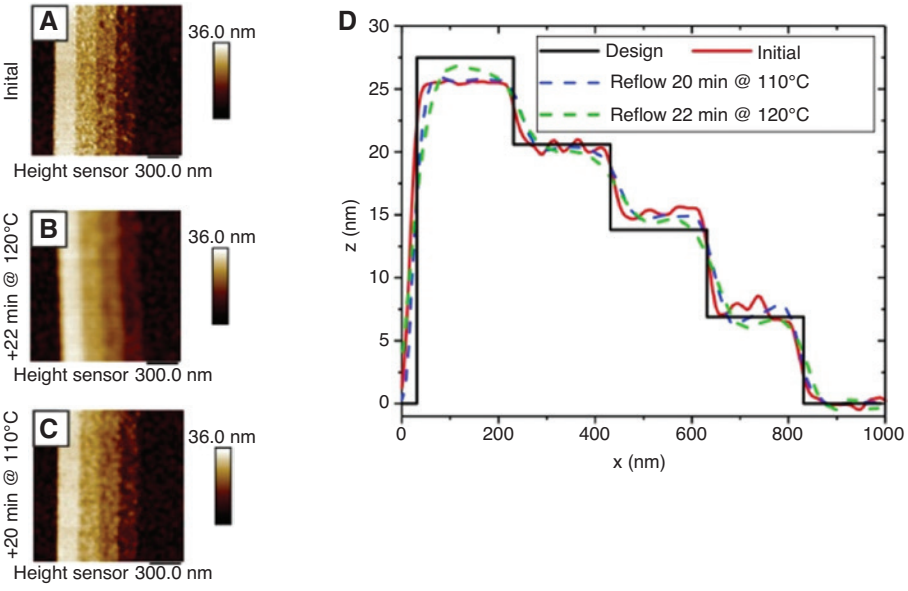

Figure 6: (A) Original profile of stepped pattern after development without further treatment and annealed profiles after (B) 22 min at 120°C and (C) 20 min at 110°C helping to reduce the surface roughness; (D) full field average of lines scans in (A)–(C).

stepped and continuous profile patterns down to sub-10-nm step height. The used low-contrast resist showed increasing limitations of the 6-nm single-step height features below 100-nm step width and reached a clear limit around 32-nm step width. Unexposed auxiliary features could significantly improve the discrete pattern definition. The surface roughness could be significantly reduced by thermal annealing and local material relocation. The line edge roughness was changed in favor of low-frequency components but needs more careful consideration when applying reflow for smoothening. After all, the presented grayscale method is well suited for direct writing of demanding diffractive optics.

Acknowledgments: The authors express their thanks to A. Schleunitz (former PSI) for initially starting the research on grayscale electron beam lithography using PMMA at PSI.

Author contributions: RK carried out the experiments, analyzed the results and wrote the manuscript. VAG optimized the electron beam writing procedure and originally had developed the gap exposure concept. HS supervised the research. All authors proofread and improved the manuscript.

References

[1] S. Landis, V. Reboud, T. Enot and C. Vizioz, Microelectron. Eng. 110, 198–203 (2013).
[2] D. C. O'Shea, T. J. Suleski, A. D. Kathman and D. W. Prather, Diffractive optics – design, fabrication, and test, SPIE, 2nd print, 133–148 (2015).
[3] H. Andersson, M. Ekberg, S. Hård, S. Jacobsson, M. Larsson, et al., Appl. Opt. 29, 4259–4267 (1990).
[4] Y. Oppliger, P. Sixt, J. M. Stauffer, J. M. Mayor, P. Regnault, et al., Microelectron. Eng. 23, 449–454 (1994).
[5] W. Däschner, P. Long, M. Larsson and S. H. Lee, J. Vac. Sci. Technol. B13, 2729–2731 (1995).
[6] W. Däschner, P. Long, R. Stein, C. Wu and S. H. Lee, Appl. Opt. 36, 4675–4680 (1997).
[7] M. T. Gale, M. Rossi, H. Schütz, P. Ehbets, H. P. Herzig, et al., Appl. Opt. 32, 2526–2533 (1993).
[8] V. V. Aristov, S. V. Dubonos, R. Y. Dyachenko, B. N. Gaifullin, V. N. Matveev, et al., J. Vac. Sci. Technol. B13, 2526–2528 (1995).
[9] D. R. S. Cumming, I. I. Khandaker, S. Thoms and B. G. Casey, J. Vac. Sci. Technol. B15, 2859–2863 (1997).
[10] Y. Hirai, S. Harada, H. Kikuta, Y. Tanaka, M. Okano, et al., J. Vac. Sci. Technol. B20, 2867–2871 (2002).
[11] Y. Shinonaga, K. Ogino, N. Unno, S. Yoshida, M. Yamamoto, et al., Microelectron. Eng. 141, 102–106 (2015).
[12] R. Kirchner, V. A. Guzenko, I. Vartiainen, N. Chidambaram and H. Schift, Microelectron. Eng. 153 633, 71–77 (2016).
[13] S. Pfirrmann, R. Kirchner, O. Lohse, V. A. Guzenko, A. Voigt, et al., Proc. SPIE 9779, 977925 (2016).
[14] S. M. Stavis, E. A. Strychalski and M. Gaitan, Nanotechnol. 20, 165302 (2009).
[15] A. F. Lasagni, S. Alamri, A. I. Aguilar-Morales, F. Rößler, B. Voisiat, et al., Appl. Sci. 8, 1260 (2018).
[16] R. Fallica, R. Kirchner, H. Schift and Y. Ekinci, Microelectron. Eng. 177, 1–5 (2017).
[17] E. R. Dufresne, G. C. Spalding, M. T. Dearing, S. A. Sheets and D. G. Grier, Rev. Sci. Instrum. 72, 1810–1816 (2001).
[18] T. Tanaka, D. Sugihara, M. Sasago, H. Kikuta, H. Kawata, et al., J. Vac. Sci. Technol. B35, 06G308 (2017).
[19] P. P. Naulleau, J. A. Liddle, F. Salmassi, E. H. Anderson and E. M. Gullikson, Appl. Opt. 43, 5323–5329 (2004).
[20] A. Flores, M. R. Wang and J. J. Yang, Appl. Opt. 43, 5618–5630 (2004).
[21] A. Schleunitz, C. Spreu, M. Vogler, H. Atasoy and H. Schift, J. Vac. Sci. Technol. B 29, 06FC01 (2011).
[22] H. Schift, Appl. Phys. A 121, 415–435 (2015).
[23] B. Radha, S. H. Lim, M. S. M. Saifullah and G. U. Kulkarni, Sci. Rep. 3, 1–8 (2013).
[24] J. A. McCoy, R. L. McEntaffer and C. M. Eichfeld, J. Vac. Sci. Technol. B36, 06JA01 (2018).
[25] S. Zhang, J. Shao, J. Liu, C. Xu, Y. Ma, et al., J. Vac. Sci. Technol. B32, 06F504 (2014).
[26] A. Schleunitz, V. A. Guzenko, A. Schander, M. Vogler and H. Schift, J. Vac. Sci. Technol. B29, 06F302 (2011).
[27] A. Schleunitz, V. A. Guzenko, M. Messerschmidt, H. Atasoy, R. Kirchner, et al., Nano Converg. 1, 1–8 (2014).
[28] V. Guzenko, N. Belić, C. Sambale, A. Schleunitz and C. David, Proc. 37th Int. Conf. on Micro and Nano Engineering, 2011 (O-LITH-40).
[29] M. Mühlberger, M. Rohn, J. Danzberger, E. Sonntag, A. Rank, et al., Microelectron. Eng. 141, 140–144 (2015).
[30] I. Khazi, U. Muthiah and U. Mescheder, Microelectron. Eng. 193, 34–40 (2018).

Robert Kirchner
Paul Scherrer Institute, Laboratory for Micro- and Nanotechnology, 5232 Villigen PSI, Switzerland; and Technische Universität Dresden, Institute of Semiconductors and Microsystems, 01062 Dresden, Germany
robert.kirchner@tu-dresden.de

Robert Kirchner studied at the Technische Universität (TU) Dresden, Germany, and Chalmers Tekniska Högskola, Göteborg, Sweden. He received his PhD in electrical engineering from TU Dresden in 2011. He worked as a postdoc at TU Dresden in 2012 and at the Paul Scherrer Institute, Switzerland, from 2013 until 2017. Since 2017, he has held a DFG Heisenberg Fellowship and is leading the Mesocopic 3D Systems Group at TU Dresden. His current research focus is on micro-nano-origami methods, 3D MEMS/NEMS, self-assembly and advanced 3D patterning methods.

Vitaliy A. Guzenko
Paul Scherrer Institute, Laboratory for Micro- and Nanotechnology, 5232 Villigen PSI, Switzerland

Vitaliy A. Guzenko studied physics at Taras Shevchenko National University of Kyiv, Ukraine. He received his PhD from RWTH Aachen University, Germany, in 2002. He worked as a postdoc in Research Centre Jülich, Germany. Since 2008, he is a staff member at the Paul Scherrer Institute, Switzerland. His research focus is on e-beam lithography and nano- and microfabrication.

Helmut Schift
Paul Scherrer Institute, Laboratory for Micro- and Nanotechnology, 5232 Villigen PSI, Switzerland

Helmut Schift obtained his diploma in electrical engineering and later his PhD in mechanical engineering from the University of Karlsruhe, Germany, in 1994, following a cooperation with the Institute of Microtechnology Mainz (ICT-IMM). Since 1994, he is a staff scientist at the Paul Scherrer Institute, Switzerland, and the head of the Polymer Nanotechnology Group (INKA-PSI). In 2011, he was a visiting professor at the Technical University of Denmark (DTU). He is a recognized pioneer of nanoimprint lithography and currently focuses on innovative polymer processing technologies.